UNCLASSIFIED

SECURITY CLASSIFICATION OF THIS PAGE

(2)

REPORT DOCUMENTATION PAGE

1a. REPORT SECURITY CLASSIFICATION UNCLASSIFIED	1b. RESTRICTIVE MARKINGS DTIC FILE COPY
2a. SECURITY CLASSIFICATION AUTHORITY AD-A211 537	3. DISTRIBUTION/AVAILABILITY OF REPORT Approved for public release; distribution is unlimited.
	5. MONITORING ORGANIZATION REPORT NUMBER(S) AFOSR-TR- 89-1186
6a. NAME OF PERFORMING ORGANIZATION Univ of Washington	6b. OFFICE SYMBOL (If applicable)
7a. NAME OF MONITORING ORGANIZATION AFOSR/NP	
6c. ADDRESS (City, State, and ZIP Code) Seattle, WA 98195	7b. ADDRESS (City, State, and ZIP Code) Building 410, Bolling AFB DC 20332-6448
8a. NAME OF FUNDING/SPONSORING ORGANIZATION AFOSR	8b. OFFICE SYMBOL (If applicable) NP
9. PROCUREMENT INSTRUMENT IDENTIFICATION NUMBER AFOSR-84-0355	
8c. ADDRESS (City, State, and ZIP Code) Building 410, Bolling AFB DC 20332-6448	10. SOURCE OF FUNDING NUMBERS

PROGRAM ELEMENT NO.	PROJECT NO.	TASK NO.	WORK UNIT ACCESSION NO.
61102F	2301	A7	

DTIC ELECTE AUG 21 1989 S C E

11. TITLE (Include Security Classification)

GRADED BANDGAP SOLAR CELLS (U)

12. PERSONAL AUTHOR(S)
Dr Larry Olsen

13a. TYPE OF REPORT	13b. TIME COVERED	14. DATE OF REPORT (Year, Month, Day)	15. PAGE COUNT
FINAL	FROM 1 Sep 84 TO 30 Sep 88	June 1989	37

16. SUPPLEMENTARY NOTATION

17. COSATI CODES			18. SUBJECT TERMS (Continue on reverse if necessary and identify by block number)
FIELD	GROUP	SUB-GROUP	
	20:12		

19. ABSTRACT (Continue on reverse if necessary and identify by block number)

This program has emphasized investigations of graded bandgap solar cells. The key objective was to determine the feasibility of obtaining high efficiencies with a graded emitter heterojunction structure. The Al(x)Ga(1-x)As ternary system was selected for actual device fabrication and characterization. Interpretation of photoresponse data for graded devices indicated that the minority carrier diffusion length was essentially zero for x equal to orgreater than .25. This property of th AlGaAs films made it impossible to obtain the expected photocurrent from the graded devices. However, studies were carried out which clearly indicated that the structures with graded emitters were characterized by an enhanced photoresponse relatice to homojunction devices. This effort resulted in the fabrication of heterofaced GaAs solar cells ehich exhibited AMI efficiencies of 21.5%.

(JST) E

20. DISTRIBUTION/AVAILABILITY OF ABSTRACT	21. ABSTRACT SECURITY CLASSIFICATION
X ☐ UNCLASSIFIED/UNLIMITED X ☐ SAME AS RPT. ☐ DTIC USERS	UNCLASSIFIED

22a. NAME OF RESPONSIBLE INDIVIDUAL	22b. TELEPHONE (Include Area Code)	22c. OFFICE SYMBOL
R J SMITH	(202) 767-4908	AFOSR/NP

DD FORM 1473, 84 MAR

83 APR edition may be used until exhausted.
All other editions are obsolete.

SECURITY CLASSIFICATION OF THIS PAGE

UNCLASSIFIED

89 8 21 097

86NP167 R 26 Jun
83NP255
Ben 86NP286

GRADED BANDGAP SOLAR CELLS

FINAL REPORT
For Work Done
9/1/84 - 9/30/88

AFOSR GRANT:	AFOSR-84-0355
START DATE:	9/1/84
CONTRACTOR:	University of Washington (Tri-Cities University Center)
PRINCIPAL INVESTIGATOR:	Dr. Larry C. Olsen

ABSTRACT

This program has emphasized investigations of graded bandgap solar cells. The key objective was to determine the feasibility of obtaining high efficiencies with a graded emitter heterojunction structure. The graded bandgap cell is designed to produce a large photocurrent at relatively a large voltage. The device involves only one N-type to P-type transition, and is therefore only a two terminal cell. The graded emitter region provides an effective field which enhances the collection of electrons and holes. The $Al_xGa_{1-x}As$ ternary system was selected for actual device fabrication and characterization. Two types of graded emitter structures were fabricated, one with a continuously graded emitter, and another with the emitter composed of discreet regions with appropriate bandgaps. Interpretation of photoresponse data for graded devices indicates that the minority carrier diffusion length was essentially zero for $x \geq .25$. This property of the AlGaAs films made it impossible to obtain the expected photocurrent from the graded devices. However, studies were carried out which clearly indicated that the structures with graded emitters were characterized by an enhanced photoresponse relative to homojunction devices. These studies suggest that once high quality AlGaAs films can be grown, efficient graded solar cells could be fabricated. A significant effort was also devoted to the development of high efficiency GaAs solar cells. This effort resulted in the fabrication of heterofaced GaAs solar cells which exhibited AM1 efficiencies of 21.5%.

TABLE OF CONTENTS

1. INTRODUCTION

One of the approaches being pursued for fabricating high efficiency solar cells involves the use of two or more cells having different bandgaps. By utilizing more than one bandgap, a photovoltaic system can be coupled to the solar spectrum in a more optimum manner than that achieved with a single homojunction cell. The most common approach to constructing a multiple cell system involves arranging devices in tandem, in order of the bandgaps, and with the largest bandgap cell receiving the incident photons.

Tandem cell systems can be constructed in two ways: by growing a monolithic stack, or by arranging the devices in a mechanical stack. With either approach, system efficiencies of 30% are considered reasonable goals. In order to obtain efficiencies of 50%, a stack of three to five cells will be required. Even if film growth technology is developed that allows the formation of a five-cell stack, it will be difficult to form the interconnecting regions without creating regions of high electron-hole recombination, or regions of high photon absorption.

An alternative cell structure which has a large limiting efficiency is that of a graded bandgap solar cell. The graded bandgap cell is designed to produce a large photocurrent at a relatively large voltage. The device involves only one N-type to P-type transition, and is therefore only a two-terminal cell. Graded bandgap solar cells are also of interest for radiation hardened devices. The graded bandgap region provides an effective field which enhances the collection of electrons and holes, even after carrier lifetimes are reduced as a result of radiation damage.

1.1 Graded Bandgap Cell Concept

The basic approach of interest in this program is depicted in Figure 1. The front surface is P-type and has a large bandgap, E_{gmax}. The bandgap in the emitter region is gradually reduced to E_{gmin} at which point a junction

INCREASED PHOTOCURRENT

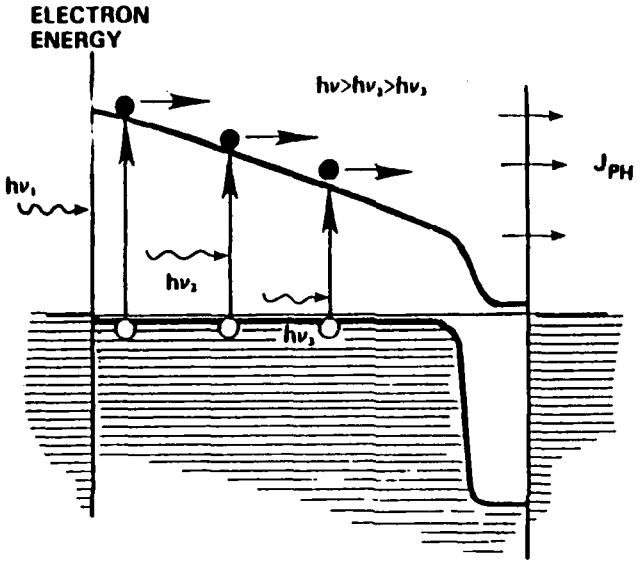

- GRADE BANDGAP TO OPTIMIZE COUPLING BETWEEN SOLAR SPECTRUM AND CELL PHOTORESPONSE
- PHOTOCURRENT CAN APPROACH THE MAXIMUM VALUE.

INCREASED VOLTAGE

(MINIMUM CARRIER RECOMBINATION)

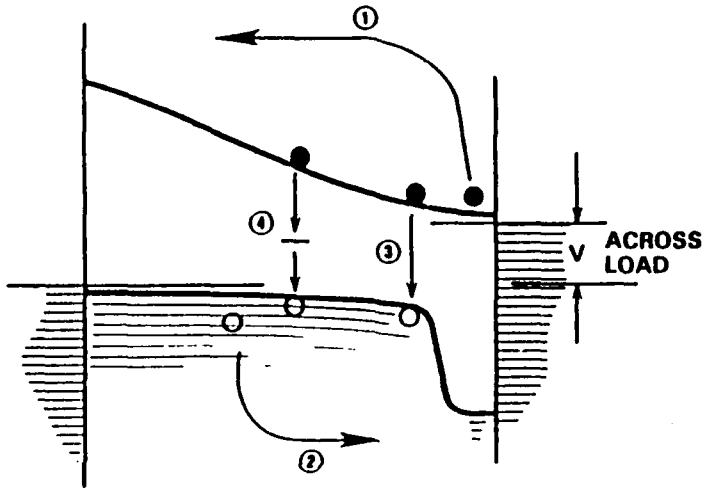

- THERMALLY ACTIVATED LOSS CURRENTS ① AND ② ARE NEGLIGIBLE BECAUSE OF LARGE BANDGAPS AT END FACES
- BAND-TO-BAND RECOMBINATION ③ REDUCED BY MINIMIZING LOW BAND GAP REGION
- RECOMBINATION VIA DEFECT ENERGY LEVELS ④ MINIMIZED BY GRADING MATERIAL COMPOSITION SUCH THAT LATTICE CONSTANT REMAINS THE SAME

Figure 1. Graded Bandgap Solar Cells: Physical Principles Under Investigation.

is formed with a large bandgap N-type region. Clearly, the order of the P-type and N-type materials can be reversed. Ideally, the variation in E_g versus x is chosen so that J_{sc} can approach the maximum value possible for E_{gmin}. In a graded structure, the front surface recombination velocity can be minimized and efficient collection of carriers from regions with a low minority carrier diffusion length can still be achieved.

A plot of the maximum value for short circuit current versus bandgap under AM0 conditions and no concentration is plotted in Figure 2. Thus, if one could utilize E_{gmin} = 1.0 eV, the maximum value of the J_{sc} is approximately 58 mA/cm^2.

If we assume that the bandgap of these two end faces is 2.5 eV, then one can estimate that the limiting value for the reverse saturation current (J_0) would be on the order of 10^{-35} A/cm^2. Assuming J_{sc}= 50 mA/cm^2, the AM1 efficiency is calculated to be significantly larger than 50%. J_0-values on the order of 10^{-35} A/cm^2 are very unlikely to be achieved. However, J_0-values less than 10^{-19} A/cm^2 have been achieved for GaAs devices. If one assumes $J_0 = 10^{-19}$ A/cm^2, efficiencies on the order of 50% are possible for graded bandgap cells. As a result, the graded bandgap cell is worthy of investigation.

1.2 Research Objectives

The overall objective of this program was to investigate the feasibility of achieving high efficiencies with graded bandgap solar cell structures. Specific objectives included: (1) fabricate graded bandgap cells based on the $Al_xGa_{1-x}As$ ternary compound system; (2) measure electro-optical properties of the devices and interpret results in terms of appropriate models; and (3) develop approaches to modeling calculations for graded bandgap cells.

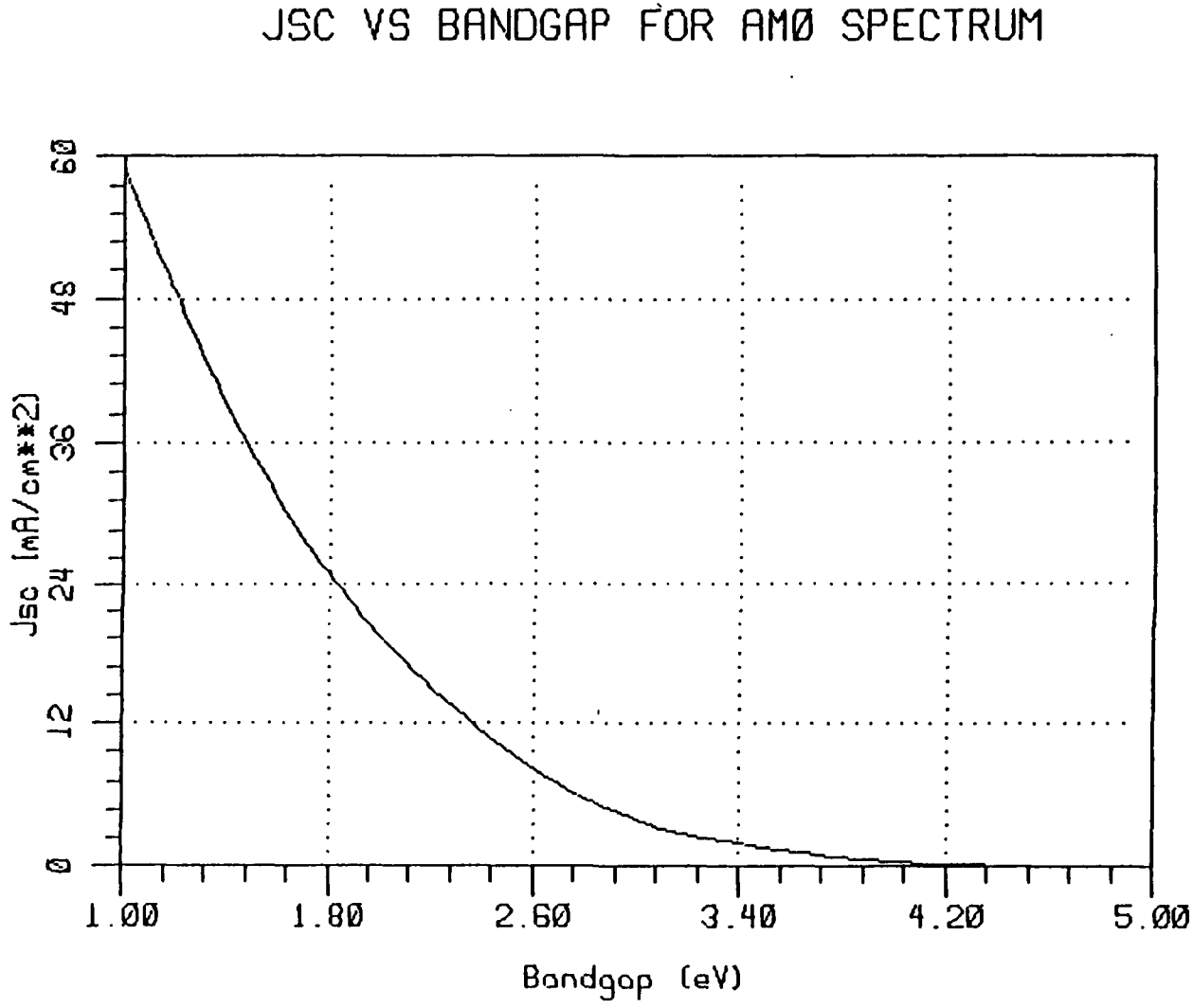

Figure 2. Maximum Short-Circuit Current versus Bandgap.

1.3 Technical Approach

Figure 3 summarizes some of the key elements of the technical approach taken in this program. Graded bandgap solar cell structures were investigated by fabricating and characterizing devices based on the $Al_xGa_{1-x}As$ materials system. As x is varied from x = 0 (GaAs) to x = 1.0 (AlAs), the bandgap changes from 1.42 eV to 2.18 eV, respectively. Throughout this composition range, the change in lattice constant is less than 1%. As a result, graded regions can be grown without the generation of misfit dislocations.

The $Al_xGa_{1-x}As$ compounds are characterized by a direct bandgap for x-values between x = 0 (E_g = 1.42 eV) and x = 0.45 (E_g = 1.96 eV). Thus, these materials are efficient optical absorbers as required for a graded solar cell. Another benefit of using the $Al_xGa_{1-x}As$ materials system for these studies is that the materials technology is relatively advanced. Multi-layered structures based on the AlGaAs system can be grown by metal organic chemical vapor deposition (MOCVD). Growth of AlGaAs by MOCVD can be purchased as a service by several industrial companies.

Solar cell studies involved an equal emphasis on studies of GaAs solar cells and graded structures. The work on GaAs cells allowed us to develop processing procedures used for high efficiency devices. The success experienced with GaAs cells indicated that procedures being used for the graded bandgap devices were adequate.

Device characterization involved photoresponse and current-voltage analyses. The photoresponse studies lead to determination of minority carrier diffusion lengths and surface recombination velocities. Current-voltage studies resulted in the identification of current loss mechanisms. Efforts to determine loss mechanisms from current voltage studies and minority carrier properties from photoresponse analyses were assisted by modeling calculations. Finally, results of device characterization and modeling calculations were used to improve device designs, procedures for MOCVD growth of films and device processing.

MATERIAL SYSTEM

- III-V COMPOUNDS
- EFFICIENT OPTICAL ABSORBERS
- ADVANCED MATERIALS TECHNOLOGY

DEVICE FABRICATION

- THIN FILM DEVICE STRUCTURES BEING FABRICATED BY METAL ORGANIC CHEMICAL VAPOR DEPOSITION.
- CONTACTS AND ANTI-REFLECTION COATINGS APPLIED BY VACUUM DEPOSITION.

DEVICE CHARACTERIZATION

- CURRENT-VOLTAGE CHARACTERISTICS, PHOTORESPONSE, DEEP LEVEL SPECTROSCOPY AND OTHER DIAGNOSTIC MEASUREMENTS ARE CONDUCTED ON CELLS.
- ELECTRO-OPITCAL CHARACTERISTICS INTERPRETED IN TERMS OF THEORY.

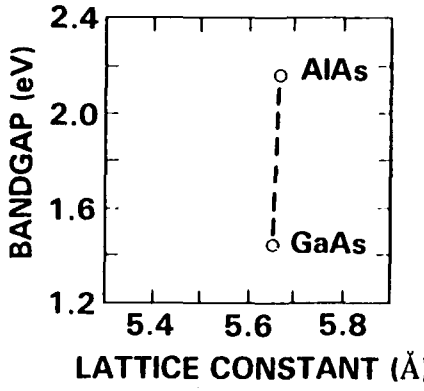

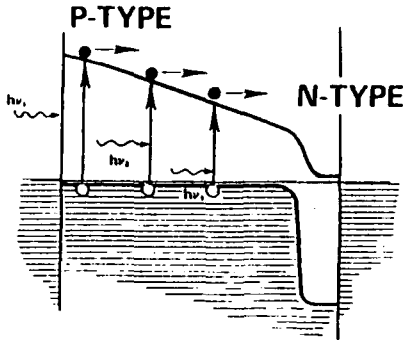

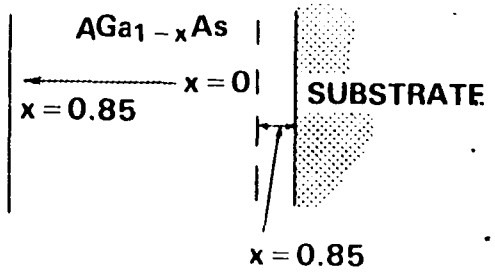

Figure 3. Graded Bandgap Solar Cells: Experimental Approach.

In the remaining sections, key results obtained from graded AlGaAs cells and GaAs solar cells are discussed.

2. GRADED BANDGAP CELL STUDIES

Two types of graded cell structures were investigated. Epi-wafers with appropriate layered structures were purchased from Spire Corporation and Epitronics. One approach was based on the use of a multilayered configuration to approximate the graded cell described by Figure 1, while the other approach involved the use of a continuously graded P-emitter as described in the figure. The results of theoretical and experimental studies are discussed in the following sections.

2.1 Graded Bandgap Cell Based on Discreet Layers

At the beginning of this program, industrial service groups could not provide graded structures based on continuously graded bandgap regions. MOCVD reactors available for service work were set up to adjust dopant concentrations and the Al/Ga ratio in discreet steps, rather than in a continuous manner. As a result, the first devices investigated in this program were based on a configuration described by Figure 4. This cell structure is described as a graded emitter heterojunction. The Al concentration, dopant concentration and other parameters of each layer are given in Table 1. A cap layer was also grown on these devices for contacting purposes. The cap layer is removed after establishing the front contacts, however. Photoresponse and current-voltage analyses are discussed in the following sections.

2.1.1 Photoresponse Studies

Internal photoresponse for a graded emitter cell is shown in Figure 11. The results were rather surprising, but consistent with conclusions concerning the GaAs homojunctions. These data can be understood by assuming the diffusion length is essentially zero in the AlGaAs layers with $x > .15$.

A theoretical model has been developed for the photoresponse of the graded emitter cell. The theory was used to fit the data shown in Figure 11 (solid line). The key assumption made in the theoretical treatment of the

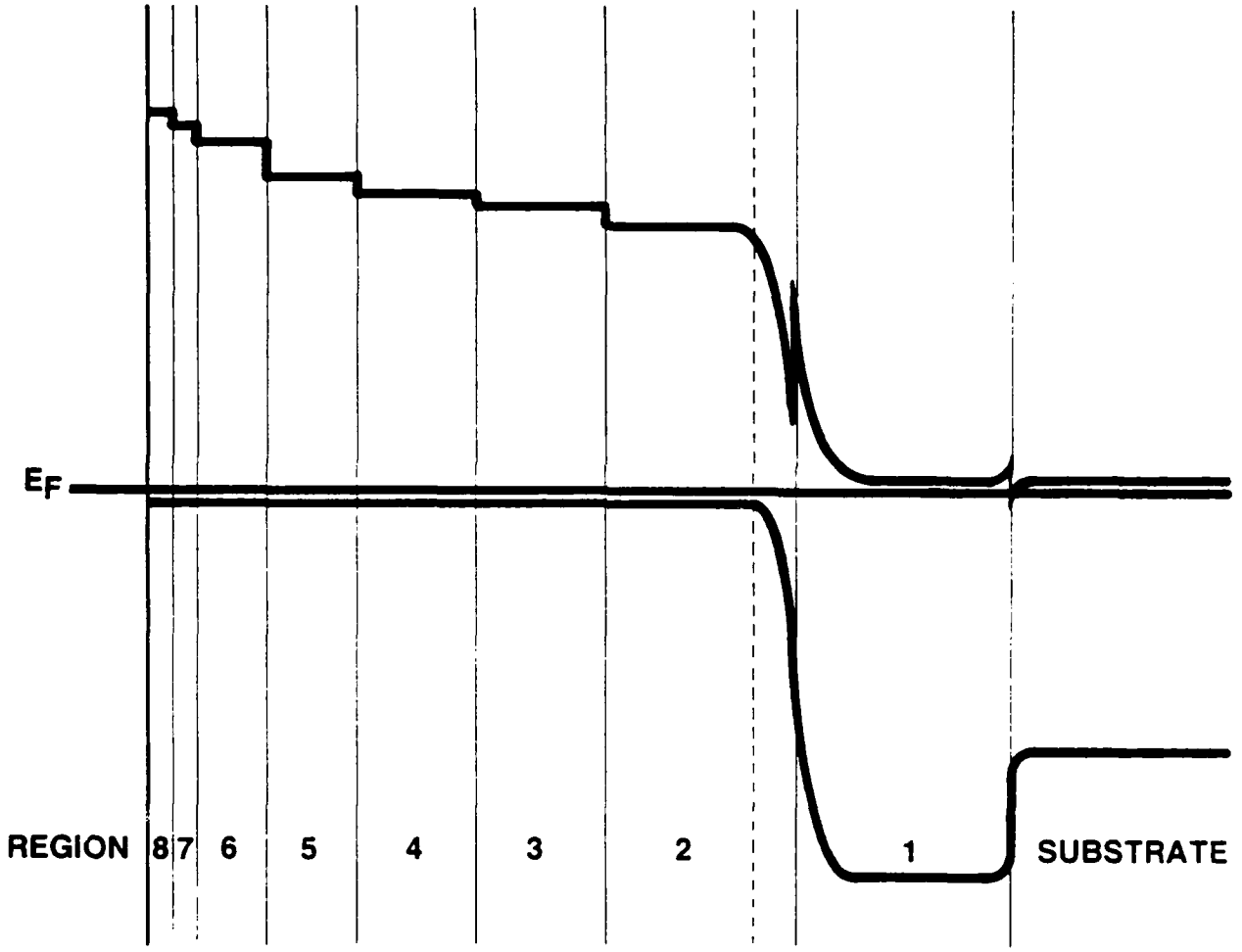

Figure 4. Electron Band Structure for Graded Emitter Heterojunction.

Table 1

PARAMETERS FOR GRADED EMITTER HETEROJUNCTION

LAYER NO.	LAYER DESCRIPTION	LAYER THICKNESS	x-VALUE IN $Al_xGa_{1-x}As$	BANDGAP	DOPANT CONCENTRATION (cm^{-3})
-	N^+-GaAs Substrate	15 mils	0	1.42	$> 10^{18}$
1	N-AlGaAs	0.1 μm	.85	2.11	10^{18}
2	P-GaAs	1.1 μm	0	1.42	10^{18}
3	P-AlgaAs	0.9 μm	.05	1.49	10^{18}
4	P-AlGaAs	0.8 μm	.15	1.61	10^{18}
5	P-AlGaAs	0.7 μm	.25	1.74	10^{18}
6	P-AlGaAs	0.4 μm	.45	1.97	10^{18}
7	P-AlGaAs	0.2 μm	.65	2.04	10^{18}
8	P-AlGaAs	0.1 μm	.85	2.11	10^{18}

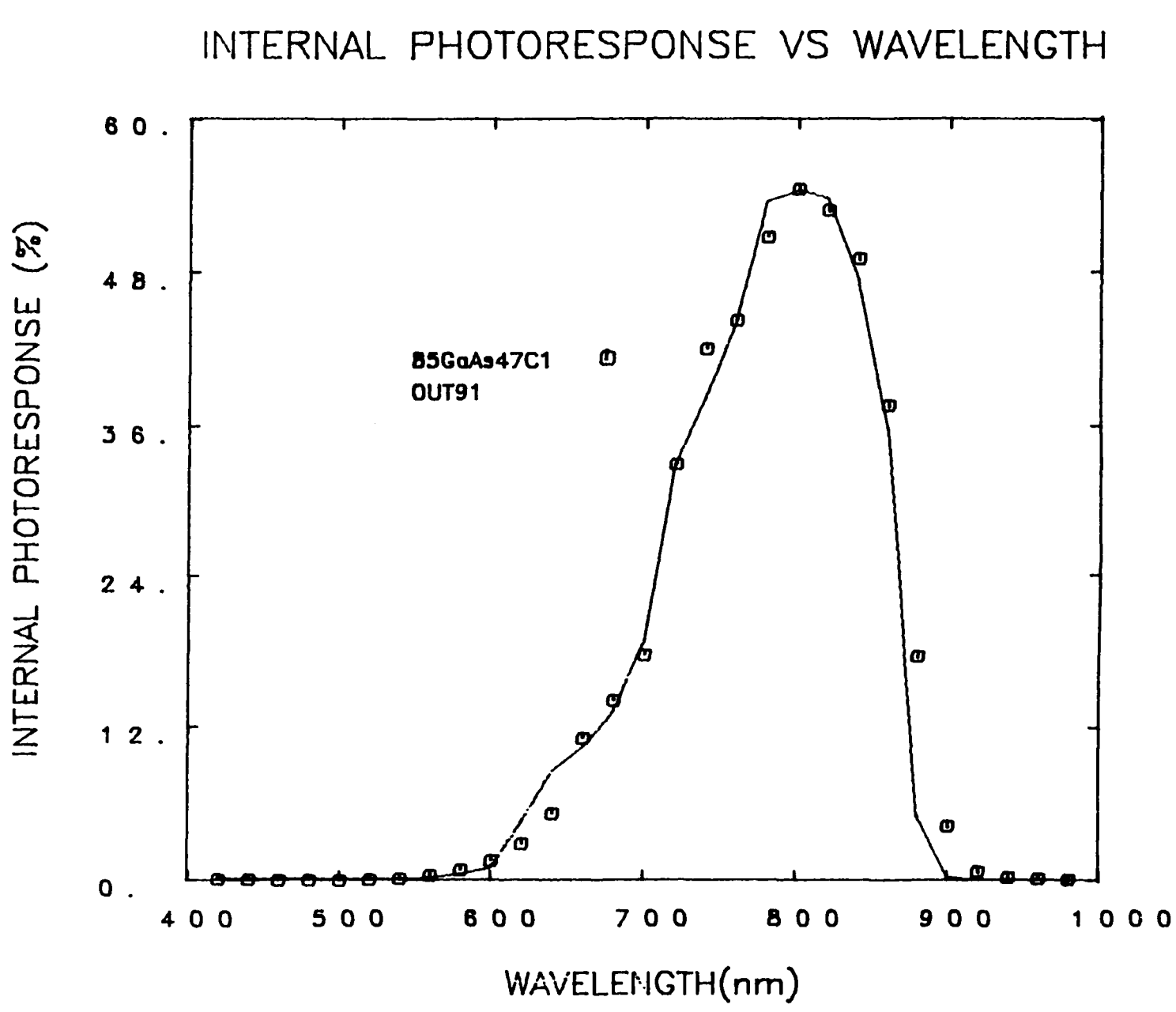

Figure 5. Internal Photoresponse for Graded Emitter Heterojunction.

Table 2

PARAMETERS DETERMINED FROM PHOTORESPONSE FOR GRADED EMITTER CELL

LAYER NUMBER	X-VALUE IN P-$Al_xGa_{1-x}As$	L_n (μm)
2	0	0.85
3	.05	0.60
4	.15	0.27
5	.25	0
6	.45	0
7	.65	0
8	.85	0

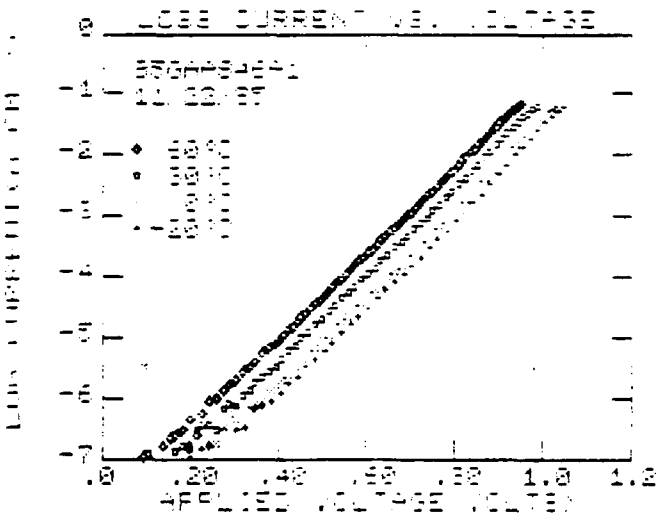

Figure 6. Current-Voltage Characteristics of Graded Emitter Heterojunctions.

problem is that if an electron moves from one layer to another going from left to right, it will be collected by the junction. The basis for this assumption is that electrons moving from left to right, an from one region to another will attain a velocity of ~ 10^7 cm/sec and should be able to escape to the right hand side of the junction.

The fit of the data for photoresponse was achieved by assuming diffusion length values as listed in Table 2. It is clear that MOCVD films of $Al_xGa_{1-x}As$ become more defective as x increases. It is suspected that the oxygen and carbon impurity concentrations increase with x.

2.1.2 Current-Voltage Analyses

Current-voltage analyses have also conducted for the graded emitter structures. Figure 12 shows typical results for these cells. The dominant current-loss in these cells can be understood in terms of multiple step tunneling. This result is consistent with the suspected high impurity concentration in the $Al_xGa_{1-x}As$ films with x = .85. Multiple-step tunneling can occur via the defects in the depletion region arising from the N-type AlGaAs layer.

These cells exhibit efficiencies on the order of 4%, mainly because the value of J_{sc} is reduced. Improvements in cell performance should result with higher quality AlGaAs layers.

2.2 Continuously Graded Structures

Figure 7 describes a graded emitter P-on-N structure. Both N-on-P and P-on-N structures were modeled as part of these studies. Graded N-on-P devices were actually fabricated and characterized. In the following sections, the modeling and experimental studies are discussed in detail.

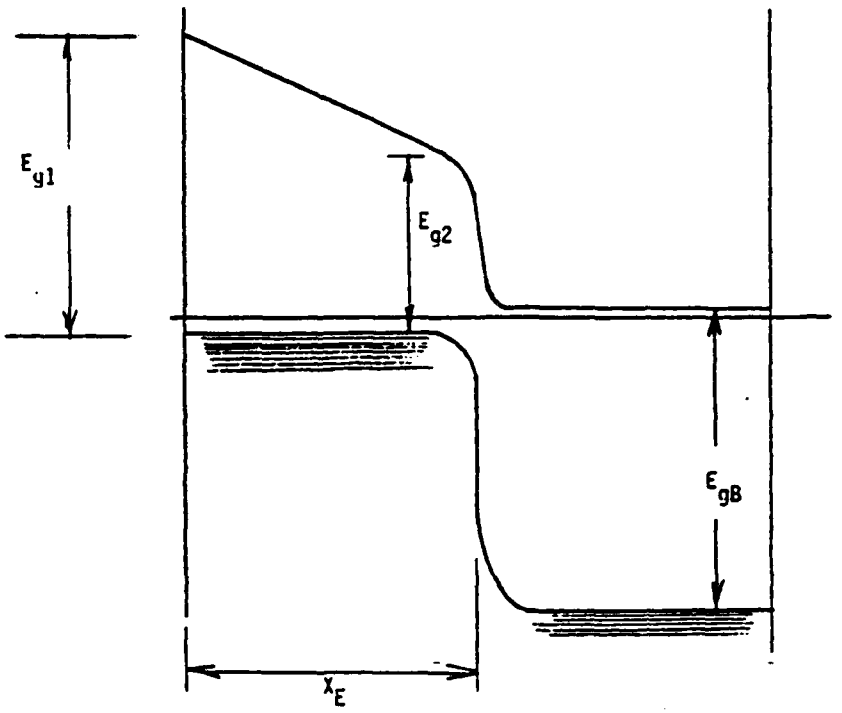

Figure 7. Electron Band Diagram for a Graded Emitter P/N Structure.

2.2.1 Modeling Calculations

Both N-on-P and P-on-N graded emitter structures have been modeled to provide guidance in cell design. The key features one must take into account in these studies are the absorption coefficient (α) versus bandgap, and the minority carrier properties of the N- and P-type materials. Our calculations all include the dependence of α on AlGaAs composition and, of course, wavelength. Although little information is available concerning the L_p for N-type AlGaAs, it seems clear that one can assume L_p is significantly less than L_n in P-type AlGaAs of the same composition.

In modeling the cell described by Figure 7, we obtain the upper limit to performance by assuming that the effective field in the emitter allows all electron-hole pairs created in the emitter to be collected. It is assumed that the P-type emitter has reasonable minority carrier properties. Thus, we can utilize a fairly wide emitter. Consider a case for which E_{g1} = 2.0 eV ($Al_xGa_{1-x}As$ with x = 0.45) with E_{g2} = 1.42 (GaAs). We assume L_n = 1 μm at the high bandgap end, and increases to L_n = 5 μm at the GaAs boundary. In order to determine the emitter thickness, it is desirable to evaluate the effect of the field $E = E_g/X_E$.

Consider the distance traveled by an electron over a period of time equal to minority carrier lifetime, τ_n. The velocity due to the field is

$$v = \mu_n E$$

The distance traveled is given by

$$\begin{aligned}(\text{Distance}) &= v\tau_n \\ &= \mu_n E\ (L^2/D_n) \\ &= \mu_n E\ (L^2/\mu_n kT/q) \\ &= EL^2/kT,\ kT \text{ in eV.}\end{aligned}$$

We can also write

$$(\text{Distance}) = E_g/X_E \; (L^2/kT)$$

with E_g and kT in eV. For L_n = 1 μm, E_g = 2.0 - 1.42 = .58 eV,

$$(\text{Distance}) = \begin{cases} 11\ \mu\text{m}, & X_E = 2\ \mu\text{m} \\ 7.5\ \mu\text{m}, & X_E = 3\ \mu\text{m} \end{cases}$$

Thus, a graded cell based on a 3 μm graded, P-type emitter should exhibit very good photoresponse.

A graded N-on-P structure presents a different situation. The value of L_p may only be 0.1 μm at the high bandgap front face of the cell. Similar considerations as above lead to the conclusion that the emitter for a N-on-P cell should be approximately 0.6 μm thick. A graded N-on-P structure is an attractive device if the P-type base is GaAs. If one desires the P-type base to have a large bandgap, say AlGaAs with E_g = 2.0 eV for voltage enhancement, then a P-on-N structure is the preferred structure.

Calculations of J_{sc} were carried out for an N-on-P structure with the P-type base being GaAs, and for a P-on-N structure with a wide bandgap base region. Results are tabulated in Table 3.

Both structures are of interest. The graded emitter, N-on-P GaAs cell may be of interest as a radiation hardened GaAs solar cell. The photoresponse of this structure benefits from both the emitter and base regions. The graded, N-type emitter should be relatively unaffected by radiation since the electron-hole pairs are collected mainly due to the effective field. The minority carrier diffusion length of the P-type base will be $\geq$ 5 μm. As a result, significant radiation damage must occur before the base contribution to current will be affected. Note that this structure has a limiting J_0-value that is the same as that for a GaAs homojunction.

The P-on-N structure has a larger potential efficiency because the limiting J_o- value is reduced because of the high bandgap, and the emitter region contribution is reduced by the effective field.

It should be emphasized that in order for these cell structures to exhibit their limiting performance, the contribution of depletion layer recombination must be minimized--that is, trap densities must be minimized. The results for J_o and V_{oc} given in Table 3 represent limiting values.

Table 3
MODELING CALCULATIONS FOR
GRADED BANDGAP SOLAR CELLS

P-ON-N

E_{g1} = 2.0 eV, E_{g2} = 1.42 eV, E_{gB} = 2.0 eV

$X_E(\mu m)$	1.5	2.0	2.5	3.0
AM1$(J_{sc})_{MAX}$	23.8	25.0	25.7	26.3
MAXIMUM AM1 EFFICIENCY (%)	24.7	25.9	26.7	27.3

N-ON-P

E_{g1} = 2.0 eV, E_{g2} = 1.42 eV, E_{gB} = 1.42 eV
L_B = 5.0 μm, X_E = 0.5 μm, X_B = 4.0 μm

$L_B(\mu m)$	2.0	5.0
AM1$(J_{sc})_{MAX}(mA/cm^2)$	28.6	30.3
MAXIMUM AM1 EFFICIENCY (%)	26.8	28.0

Comments: For P/N:

(1) Due to effective field, $J_o \simeq 10^{-22}$ A/cm^2 and $V_{oc} \simeq 1.22$ volts.

(2) For N/P: $J_o \simeq J_{oB} \simeq 10^{-19}$ A/cm^2
$V_{oc} \simeq 1.04$ volts.

(3) Auger recombination is not taken into account.

2.2.2 Graded AlGaAs Solar Cells

Cell Design and Fabrication--In order to study the effect of a graded bandgap emitter, two cell structures were fabricated, an AlGaAs homojunction, and a similar cell except that the emitter composition was graded. The electron band diagrams for the two devices are depicted in Figure 8. Other details such as dopant concentrations, layer thicknesses and layer compositions are given in Tables 4 and 5. N-type emitters were used so that an adequate sheet conductance could be obtained.

Photoresponse of AlGaAs Cells--Internal photoresponse data shown in Figure 9 for the two types of AlGaAs cells illustrate in a rather dramatic fashion the effect of a graded bandgap emitter. The quantum efficiency of the graded emitter cell is greater than that of the homojunction cell by a factor of four. Analysis of the homojunction photoresponse revealed that the minority carrier diffusion lengths in both the N-type emitter and P-type base are very short. Thus, a graded emitter appears necessary for a cell based on $Al_xGa_{1-x}As$ with $x \simeq 0.25$.

Computer aided analyses of the homojunction photoresponse data were carried out. Figure 10 shows the best fit to the experimental data. The parameters corresponding to the best fit are:

Surface Recombination Velocity of the Front Surface, S(F)	$> 10^4$ cm/sec
Surface Recombination Velocity of the Back Surface, S(B)	$> 10^4$ cm/sec
Minority Carrier Diffusion Length for Emitter, L(F)	$= 0.03$ μm

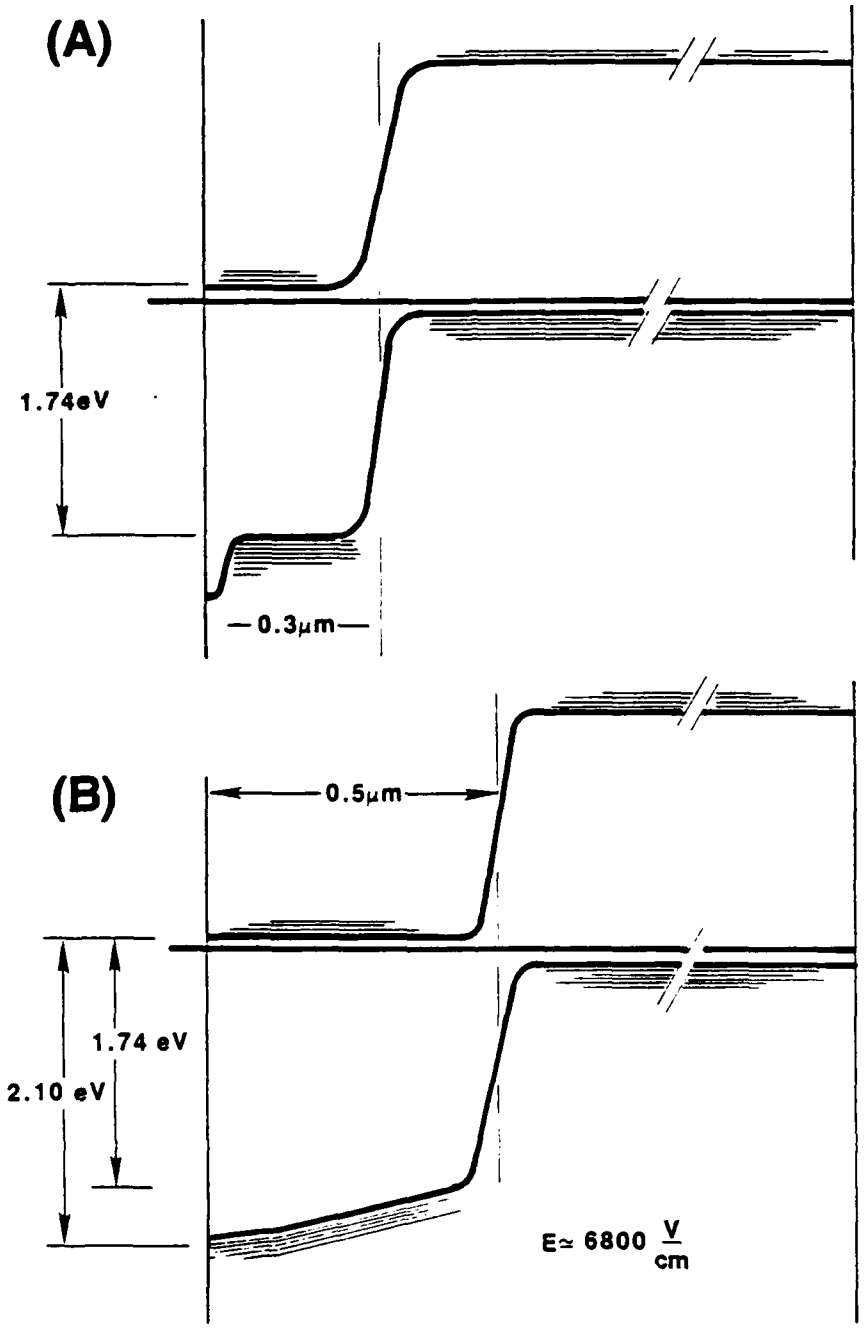

Figure 8. Electron Band Diagram for (A) AlGaAs Homojunction and (B) AlGaAs Graded Emitter Solar Cell.

Table 4

SPECIFICATIONS FOR GRADED AlGaAs HOMOJUNCTION SOLAR CELL

LAYER NUMBER	LAYER DESCRIPTION	DOPANT CONCENTRATION (cm^{-3})	LAYER THICKNESS (μm)
6	N^+-GaAs (Cap)	1×10^{18}	0.1
5	N-$Al_{.90}Ga_{.10}As$	$1\text{-}2 \times 10^{18}$	.05
4	N-$Al_{.25}Ga_{.75}As$	$1\text{-}2 \times 10^{18}$	0.3
3	P-$Al_{.25}Ga_{.75}As$	$1\text{-}2 \times 10^{18}$	3.0
2	P-$Al_{.90}Ga_{.10}As$	$1\text{-}2 \times 10^{18}$	0.1
1	P-GaAs (BUFFER LAYER)	$1\text{-}2 \times 10^{18}$	1.0
SUBSTRATE	P^+GaAs (CLASS A SUMITOMA)	$> 10^{18}$	

Table 5

SPECIFICATIONS FOR GRADED AlGaAs SOLAR CELL

LAYER NUMBER	LAYER DESCRIPTION	DOPANT CONCENTRATION (cm^{-3})	LAYER THICKNESS (μm)
5	N^+-GaAs (CAP)	$> 1 \times 10^{18}$	0.1
4 (GRADED)	N-$Al_{.90}Ga_{.10}As$ / N-$Al_{.25}Ga_{.75}As$	$1\text{-}2 \times 10^{18}$	0.5
3	P-$Al_{.25}Ga_{.75}As$	$1\text{-}2 \times 10^{18}$	3.0
2	P-$Al_{.90}Ga_{.10}As$	$1\text{-}2 \times 10^{18}$	0.1
1	P-GaAs (BUFFER LAYER)	$1\text{-}2 \times 10^{18}$	1.0
SUBSTRATE	P^+GaAs (CLASS A SUMITOMA)	$> 10^{18}$	

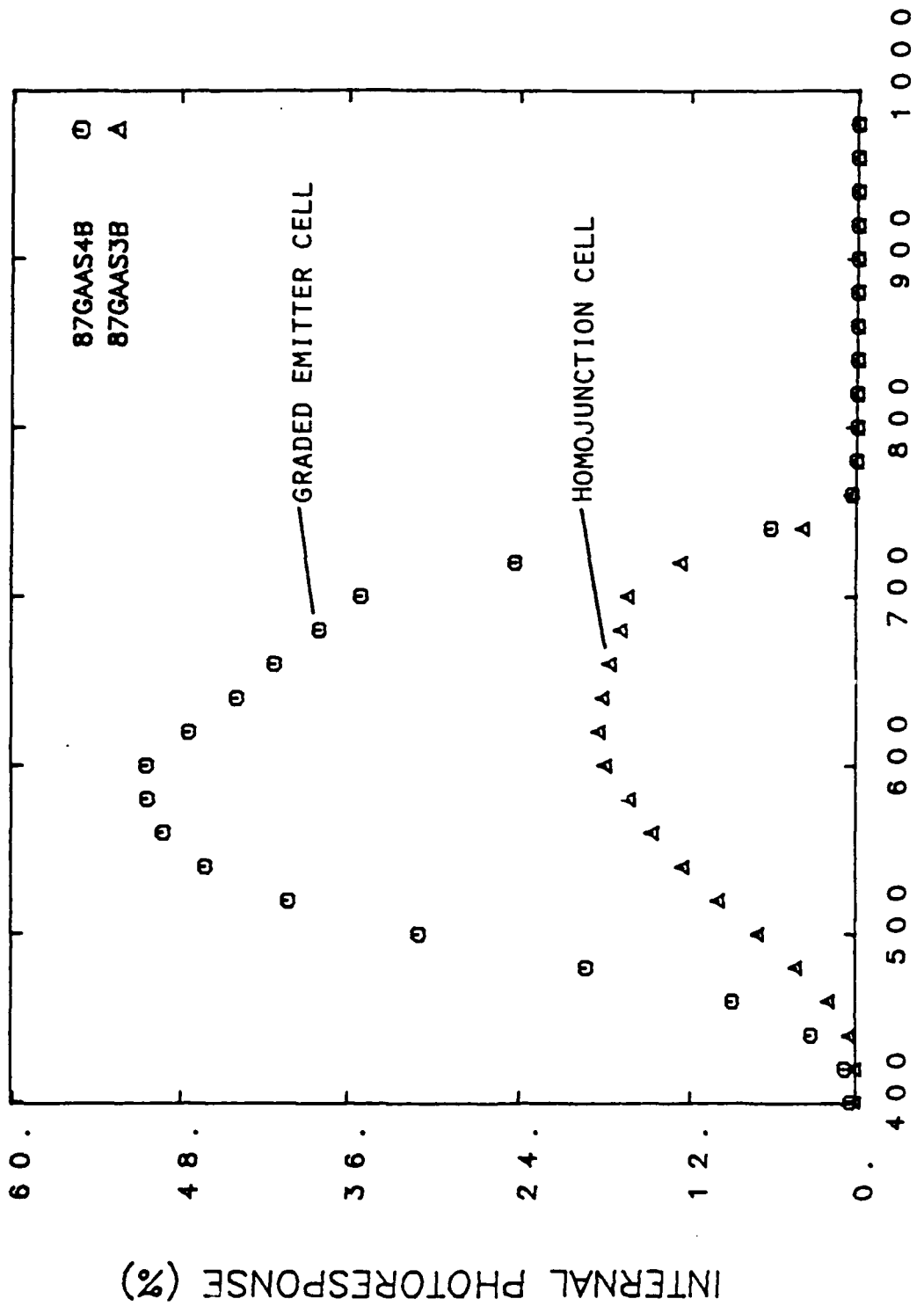

Figure 9. Internal Photoresponse Determined for A[illegible] Graded Emitter and Homojunction Solar Cells.

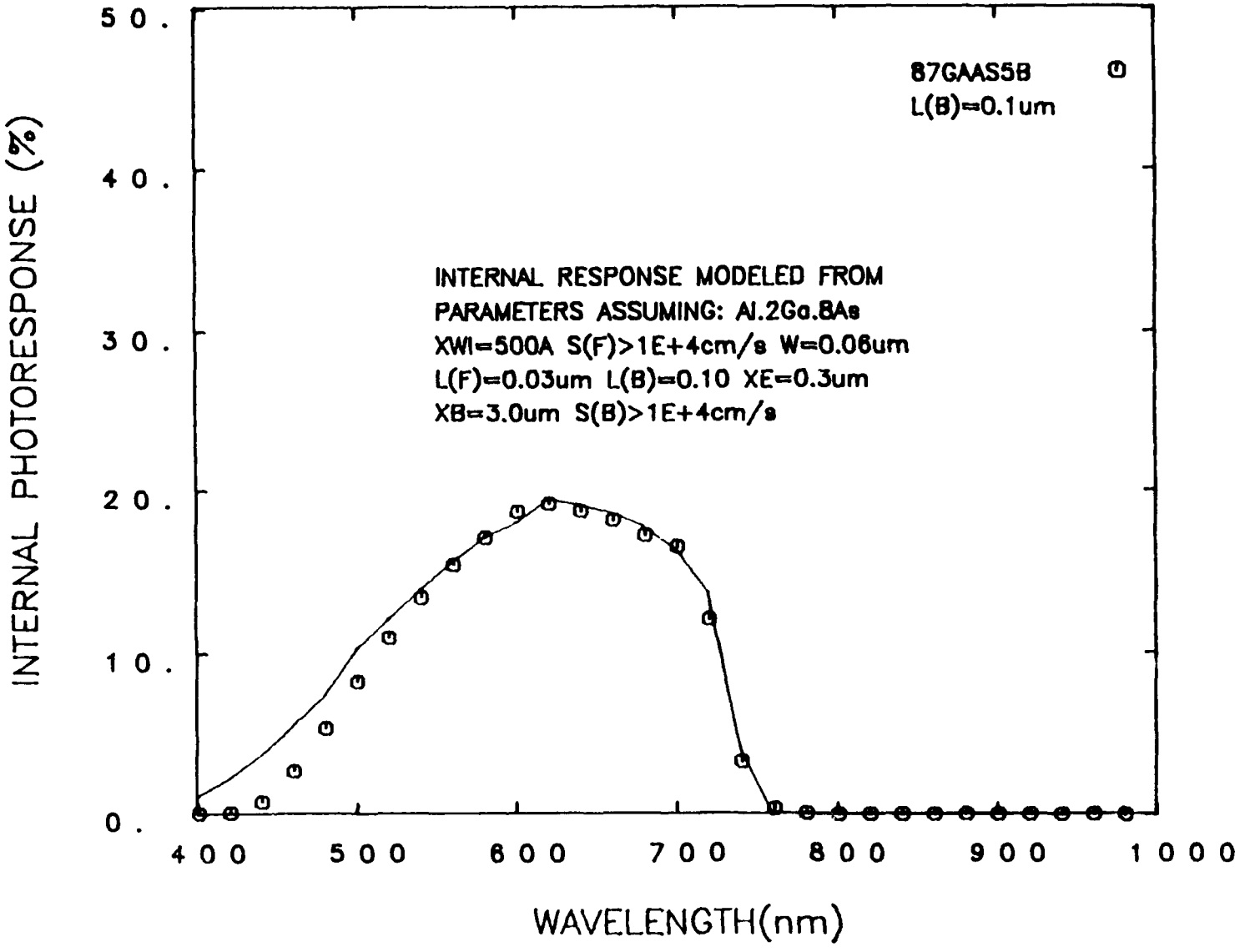

Figure 10. Internal Photoresponse Data and Theoretical Fit of Data for AlGaAs Homojunction Solar Cell.

Minority Carrier Diffusion Length for Base, L(B)	= 0.10 μm

The key results are the values obtained for L(F) and L(B).

The emitter diffusion length is very close to zero. If one assumes that L(F) and L(B) have similar values in the graded emitter cell, it is clear that the large difference in tne photoresponse values is due to enhanced emitter collection that results from the effective built-in electric field.

The value obtained for L(B) is surprisingly low. These layered structures were grown by Epitronics. It appears that the $Al_xGa_{1-x}As$ layers are very defective. Larger diffusion lengths have been measured for P-type AlGaAs layers by researchers at Varian. However, it is generally assumed that N-type AlGaAs layers are characterized by low diffusion lengths.

3. GaAs SOLAR CELL STUDIES

Investigations of GaAs heteroface solar cells were conducted in an effort to develop processing techniques with cells that are also being studied by other research groups. Fabrication procedures developed for GaAs cells are clearly relevant to graded bandgap cells based on the $Al_xGa_{1-x}As$ materials system.

In addition to developing fabrication procedures appropriate for AlGaAs cells, we also attempted to understand basic mechanisms which limit the performance of GaAs solar cells. The approach utilized involved conducting photoresponse and temperature dependent current-voltage measurements, and interpretation of the data in terms of theory to determine key device parameters.

3.1 Cell Fabrication and Performance

GaAs solar cell structures studied in this work are described by Figure 11 and Table 6. The basic layered structures were grown by MOCVD according to our specification by industrial suppliers. Cells were then fabricated using processing steps which included metallization, mesa formation, cap removal, and AR layer deposition. These studies resulted in numerous cells which exhibited AM1.5 efficiencies in the range of 21 to 22%. Illuminated I-V characteristics measured by SERI are shown in Figure 12. These cells are nominally 1.5 X 1.5 cm in size.

The efficiencies achieved in this program are less than those reported in Reference 1, namely, the 23.7% for a 0.25 cm^2 by Tobin, et al. The major reason for the larger efficiency of the Spire cell is that they achieved a J_{sc}-value of 27.75 mA/cm^2. The cells fabricated in this effort were characterized by J_{sc}-values on the order of 24.9 mA/cm^2.

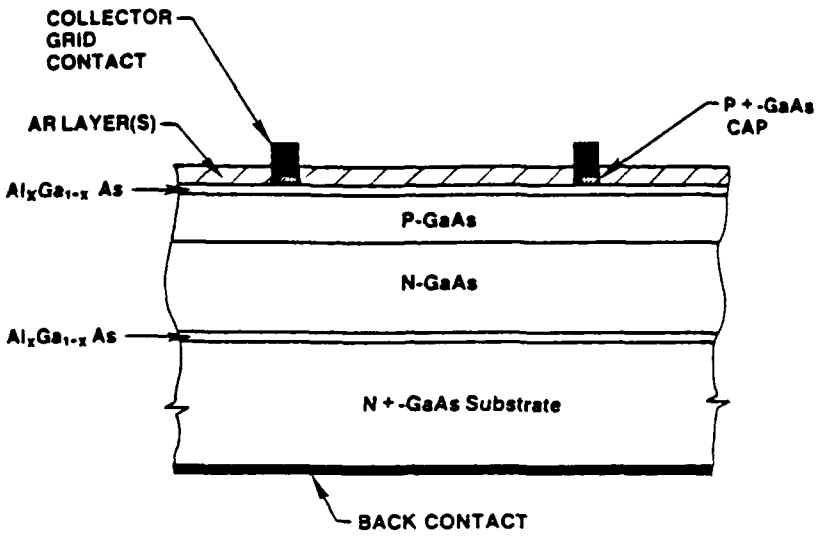

Figure 11. GaAs Solar Cell Structure (See Table 1 for Other Information).

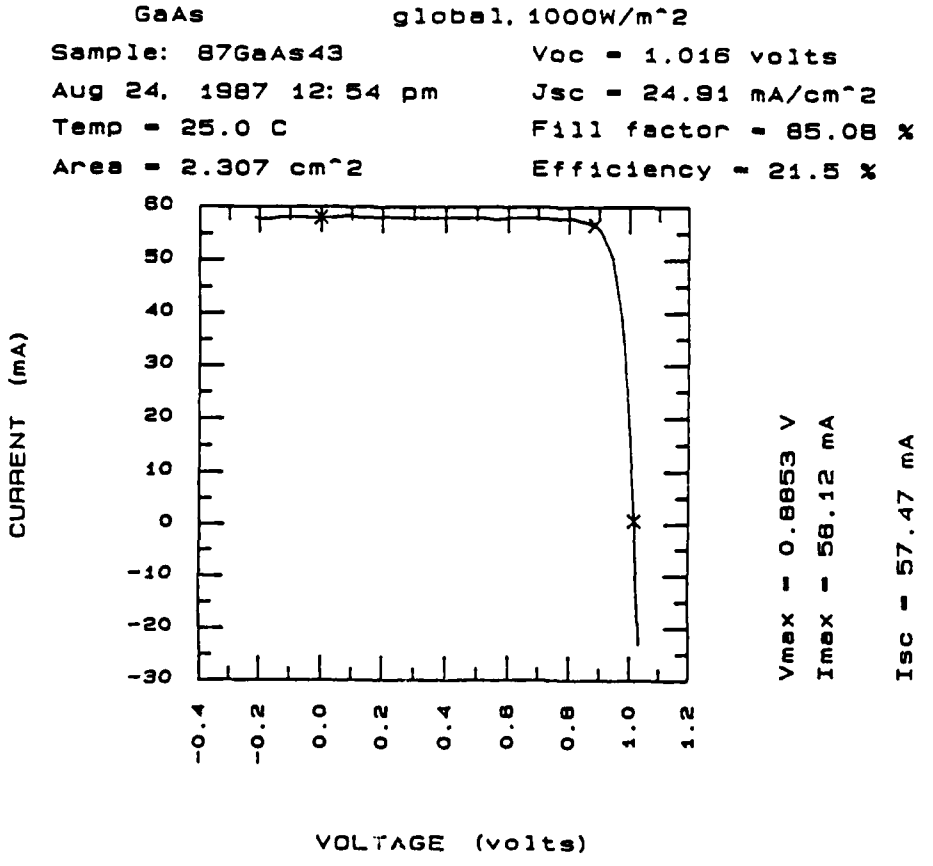

Figure 12. Illuminated Current-Voltage Characteristics Measured by the Solar Energy Research Institute.

Table 6

GaAs CELL STRUCTURE

LAYER	ALUMINUM CONCENTRATION (%)	DOPANT CONCENTRATION (cm^{-3})	THICKNESS (μm)
P^+ GaAs CAP	-	Zn: >3E18	0.1
P-AlGaAs WINDOW	90%	Zn: 1E18	.05
P-GaAs EMITTER	-	Zn: 1E18	0.5
N-GaAs BASE	-	Si: 3E17	3.0
N-AlGaAs REFLECTOR	90%	Si: 1E18	0.1
N-GaAs BUFFER	-	Si: 1E18	0.5
N-GaAs SUBSTRATE	-	Si: >1E18	-

OTHER LAYERS: AR COATING - SiN_x
FRONT METALLIZATION - Au
BACK METALLIZATION - A[illegible]Sn

During the course of this program, the efficiencies of GaAs solar cells fabricated at the Center gradually increased from a few percent to 22%. The increase in efficiency resulted from first characterizing current losses, and then modifying cell design to reduce these losses. In the following sections, results of photoresponse and current-voltage analyses are discussed.

3.2 Photocurrent Analysis

Internal photoresponse data of a typical cell exhibiting an AM1.5 efficiency in the range of 21 to 22% are shown in Figure 13. These data have been interpreted in terms of a model described by Figure 14. We find that the data can be fit quite well if one assumes that a layer of GaAs adjacent to the AlGaAs heteroface is "dead" as far as minority carrier lifetime is concerned. This layer (3A in Figure 14) is referred to as a "dead layer." The layer absorbs photons to generate electron-hole pairs, but none of the carriers are collected as current--i.e., the minority carrier lifetime is zero.

The internal photoresponse data are fit quite well by assuming the following:

GaAs Dead Layer = 70 A to 100A
Front Surface Recombination Velocity (S_F) = 10^4 cm/sec
Minority carrier Diffusion Length in the Emitter (L_E) = 5 μm
Minority Carrier Diffusion Length in the Base (L_B) - 3 μm

Detailed studies of photon carrier losses have been carried out for the cells. Significant gains in photocurrent will be obtained by accomplishing the following:

(i) Decrease S_F to 10^3 cm/sec (1.0 mA/cm^2)
(ii) Eliminate GaAs dead layer (0.6 mA/cm^2)
(iii) Decrease AlGaAs layer to 250 A (0.8 mA/cm^2)
(iv) Apply a MgF_2/ZnS double layer AR coating (1.2 mA/cm^2)

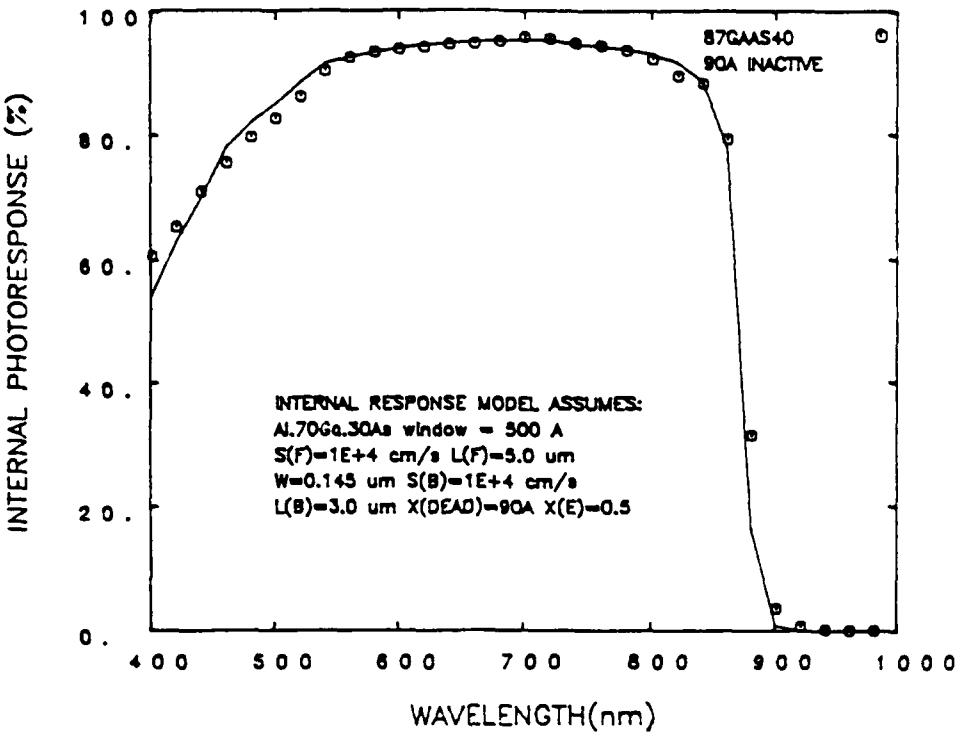

Figure 13. Internal Photoresponse for High Efficiency GaAs Solar Cell.

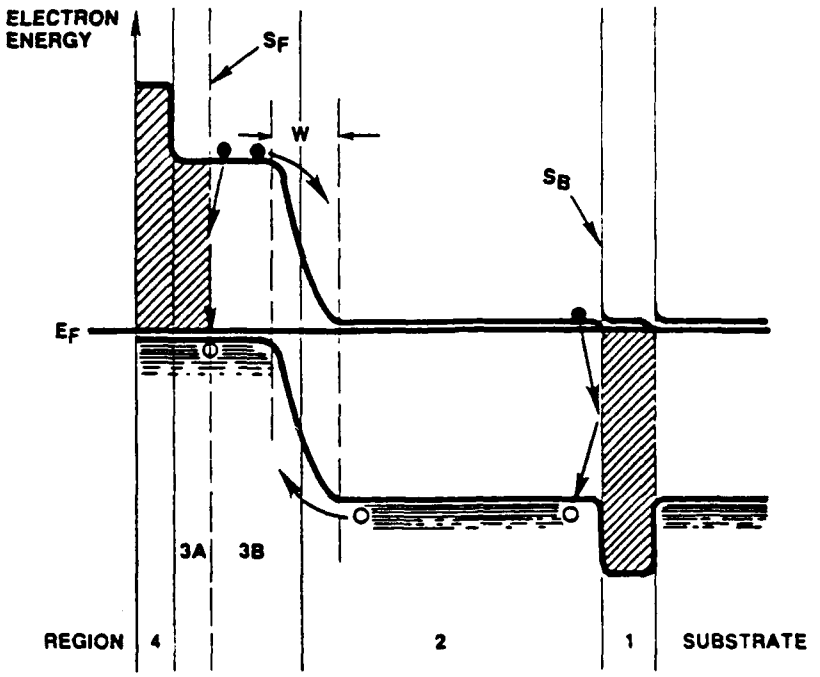

Figure 14. Electron Band Structure of Model Used to Fit Photoresponse Data. Layer 3A is the "Dead Layer."

These improvements would increase the active area photocurrent to 30.0 mA/cm^2, compared to the maximum value of 31.6 mA/cm^2. The corresponding cell efficiency would increase above 26%.

A key result of the photoresponse studies is that a dead layer approximately 20 A to 100 A thick exists in the GaAs material adjacent to the AlGaAs/GaAs interface. The approach to growth of AlGaAs on top of GaAs typically involves a change in temperature and a delay in time. While waiting for the temperature to rise from 700° C to 800° C, AsH_3 flows across the GaAs surface. It is quite plausible to expect increased incorporation of oxygen and carbon impurities at this interface due to the time delay.

3.3 Current Loss Mechanisms

Current loss mechanisms were investigated by measuring dark I-V characteristics versus temperature and interpreted in terms of theory. The procedure used in these investigations is discussed in Reference 2. It was determined that dark I-V characteristics can typically be interpreted in terms of two current mechanisms acting in parallel,

$$J = J_1 + J_2$$

Each of the current components can be expressed as

$$J_1 = J_0 \exp(CV)$$

$$J_0 = J_{00} \exp(-\phi/kT)$$

Values for C and ϕ allow one to identify the nature of the current loss mechanism. Values for C and ϕ for important current loss mechanisms are:

Emitter and Base Recombination:

$C = 1/nkT \quad n = 1.0$

$\phi = E_{go}$, where $E_g = E_{go} - aT$

$E_{go} = 1.52$ eV for GaAs

Depletion Layer Recombination:

$C = 1/nkT \quad n = 1.0$ to 2.0

$\phi = 0.5\ E_g$ to E_g

Multiple Step Tunneling:

$C = B$ = Constant Independent of Temperature

$\phi = 0$ to $E_g/2$

Figures 15 and 16 show I-V data taken at various temperatures. Cell 85-50 and 87-22 were fabricated in 1985 and 1987, respectively. The approach to analyzing these data involves fitting each set of I-V data at a given temperature in terms of a model based on two current components acting in parallel. The values of J_0 versus Temperature are then examined to determine the values of C and ϕ, and thus identify the nature of the current loss mechanism.

Results for several cells are given in Table 7. The cells listed illustrate the fact that our GaAs cells gradually improved throughout the life of this program. Typically, I-V data can be fit very well with two mechanisms, one dominant in the 0.4 to 0.8 V range, and one dominant in the 0.8 to 1.1 V range. These two voltage ranges are referred to as the low and high ranges. In 1985, cell I-V data were often characterized by two multiple step tunneling mechanisms. As device performance improves, current loss mechanisms will evolve from the tunneling process to depletion region recombination, and then to emitter/base recombination (minority carrier injection). As we progressed in developing processing techniques, and doping concentrations, the current losses were gradually reduced, until the high voltage mechanisms approached minority carrier injection, and the low voltage mechanism approached depletion region recombination, as exhibited by Cell 87-43.

As a result of various experiments, we attribute the low voltage loss mechanism in Cell 87-43 as being a result of recombination of electron-hole pairs at the device periphery. Therefore, further increase in GaAs cell performance can be achieved by improving the passivation of the device edges.

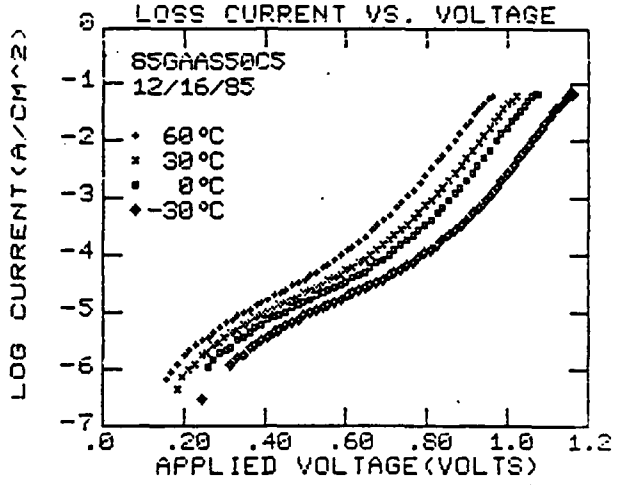

Figure 15. T-I-V Data for Cell 85GAAS50

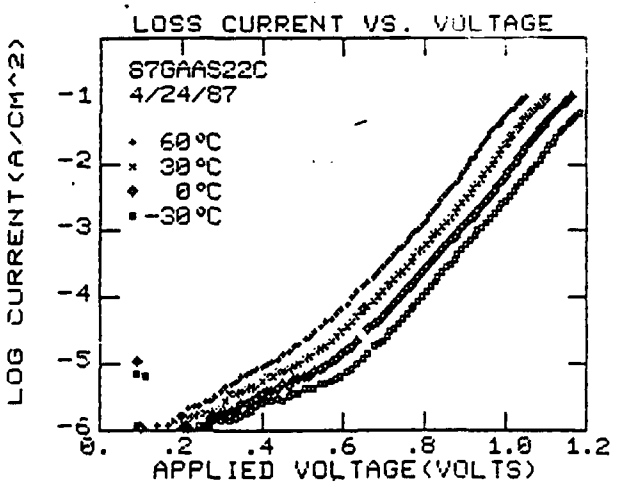

Figure 16. T-I-V Data for Cell 87GAAS22

Table 7

I-V PARAMETERS FOR GaAs SOLAR CELLS

CELL	LOW VOLTAGE RANGE				HIGH VOLTAGE RANGE			
	J_o (A/cm^2)	B (N)	ϕ (eV)	MECH	J_o (A/cm^2)	N	ϕ (eV)	MECH
85-50	6.5 E-8	9.9 (3.9)	0.1	MULT STEP TUN	2E-13	1.53	0.22	MULT STEP TUN
86-9	1E-10	16 (2.41)	0.62	MULT STEP TUN	2E-17	1.08	1.3	DEPL REGION RECOMB
87-22	2E-9	15 (2.57)	0.24	MULT STEP TUN	6E-20	1.00	1.50	EMITTER & BASE RECOMB
87-43	9.5E-12	19.2 (2.0)	0.71	DEPL REGION RECOMB	3.4E-19	1.01	1.55	EMITTER & BASE RECOMB

4. CONCLUSIONS

This program has emphasized investigations of graded bandgap solar cells. The key objective was to examine the potential for obtaining high efficiencies with a graded emitter heterojunction structure (Figure 1). The $Al_xGa_{1-x}As$ ternary system was selected for actual device fabrication and characterization.

Two types of graded structures were fabricated, a P-on-N graded emitter heterojunction with the base region having a bandgap on the order of 2.0 eV, and a N-on-P graded emitter heterojunction with the base region being GaAs. The emitter of the P-on-N structure was composed of seven regions, each having a constant bandgap. This device structure is relatively straightforward to analyze. Interpretation of photoresponse data leads to the conclusion that the minority carrier diffusion length was zero for $Al_xGa_{1-x}As$ regions with $x > .25$. This result clearly established that the quality of AlGaAs films for $x = .25$ had to be improved before an efficient graded cell could be fabricated.

The graded N-on-P structures were fabricated along with AlGaAs homojunctions in order to verify that an enhanced photoresponse could be obtained with a graded structure. Indeed a significant enhancement was observed. The efficiency of the N-on-P structure was reduced because of difficulty in contacting N-type material. Further work would be needed in order to improve the performance of this type of device.

A significant effort was devoted to development of GaAs heteroface solar cells. The primary reason for this effort was to develop processing procedures that were also pertinent to fabricating graded structures. This effort resulted in the fabrication of GaAs cells that exhibited AM1 efficiencies of 21.5%. This result was confirmed by the Solar Energy Research Institute. At the time of the achievement, the result represented one of the best results in the world.

REFERENCES

1. S.P. Tobin, et al, "A 23.7 Percent Efficient One-Sun GaAs Solar Cell," Conf. Proc. 19th IEEE Photovoltaic Specialists Conference, page 1492 (1987).

2. L.C. Olsen, et al, "Measurement and Analysis of Solar Cell Current-Voltage Characteristics," Proc. 18th IEEE Photovoltaic Specialists Conference, page 732 (1985).

Appendix A

CONTRIBUTORS TO THE PROGRAM

Dr. Larry C. Olsen - Principal Investigator. Professor of Materials Science and Engineering.

Dr. F.W. Addis - Research Scientist. Key person in device fabrication and solar cell characterization.

Glen Dunham - Research Engineer. Contributed to device fabrication and cell measurements.

Dan Huber - Graduate Student in Materials Science and Engineering.

Dave Daling - Graduate Student in Materials Science and Engineering.

Eric Eichelberger - Graduate Student in Materials Science and Engineering.

Appendix B

STUDENT DEGREES AND THESES

Eric E. Eichelberger	M.S. Materials Science and Engineering, 1985.
Thesis Title:	"Investigation of Solar Cells Based on MOCVD Multilayer AlGaAs Structures"
Daniel A. Huber	M.S. Materials Science and Engineering, 1987.
Thesis Title:	"Graded Bandgap Aluminum Gallium Arsenide Solar Cells." Now working on Ph.D. thesis.

Appendix C

PUBLICATIONS

"Electro-Optical Characterization of GaAs Solar Cells," presented at 8th Space Photovoltaic Research and Technology Conference, NASA Lewis, October 7-9, 1985 (proceedings to be published)

"Electro-Optical Characterization of GaAs Solar Cells," Proceedings 19th IEEE Photovoltaic Specialists Conference, page 238, (1987).

"Investigation of High Efficiency GaAs Solar Cells," Presented at the Space Photovoltaic Research and Technology Meeting at NASA Lewis Research Center, Cleveland, Ohio, April 19-21, 1988.

In Preparation

"Effect of 'Dead Layer' on GaAs Solar Cell Photoresponse"

"Current Loss Mechanisms in High Efficiency GaAs Solar Cells"